**Scheme II**

$$W_2(CO)_{10}^{2-} \overset{h\nu}{\rightleftharpoons} 2W(CO)_5^-$$

$$W(CO)_5^- + PR_3 \rightleftharpoons W(CO)_5PR_3^- \quad (19e^-)$$

$$W(CO)_5PR_3^- + S \rightarrow W(CO)_5PR_3 + S^-$$

S = reducible substrate

with the facts that other 17-electron radicals react with ligands to form 19-electron complexes[4-8] and that the only organometallic product formed in the reduction reactions is $W(CO)_5PR_3$. The mechanism in Scheme II is also reasonable on thermodynamic grounds because the 19-electron $W(CO)_5PR_3^-$ complexes will be very powerful reductants. Although the exact oxidation potentials are not known, values around 2.6 V vs SCE can be approximated.[51] This potential is sufficient to reduce $CO_2$.

**Summary.** In general, the photochemistry of the $W_2(CO)_{10}^{2-}$ complex is comparable to that of other metal-metal-bonded carbonyl dimers. Irradiation into the low-energy tail ($\lambda > 420$ nm) of the $d\pi \rightarrow \sigma^*$ electronic transition of the $W_2(CO)_{10}^{2-}$ complex leads to W-W bond homolysis. The resulting 17-electron $W(CO)_5^-$ radicals can be trapped with suitable ligands such as 4-cyanopyridine to give 19-electron adducts. It is proposed that ligands such as $PPh_3$ and $PBu_3$ also react with photogenerated $W(CO)_5^-$ to form adducts, $W(CO)_5PR_3^-$. These latter adducts are powerful reducing agents, and we demonstrated the reduction of several substrates, including $CO_2$, using these species. The reducing agents generated by irradiation of the $W_2(CO)_{10}^{2-}$ complex are better reductants than those generated from other metal-metal-bonded dimers such as $Cp_2Mo_2(CO)_6$.

**Acknowledgment** is made to the National Science Foundation and to the Air Force Office of Scientific Research for the support of this work. We thank Prof. N. J. Cooper and Dr. M. R. M. Bruce for helpful discussions. D.R.T. acknowledges the Alfred P. Sloan Foundation for a Fellowship.

(51) The reduction potential of $W(CO)_6$ is about -2.6 V vs SCE; that for $W(CO)_5PPh_3$ should be similar. See: Pickett, C. J.; Pletcher, D. *J. Chem. Soc., Dalton Trans.* **1975**, 879-886.

Contribution from the Department of Chemistry and the Laboratory for Surface Studies, University of Wisconsin—Milwaukee, Milwaukee, Wisconsin 53201

# Interactions of Nickel and Manganese Carbonyls with Oxide Surfaces: Formation of Reduced, Oxidized, and Zerovalent Metal Species

Michael P. Keyes, Liz U. Gron, and Kenneth L. Watters*

*Received January 28, 1988*

Reactions of the metal carbonyls $Ni(CO)_4$ and $Mn_2(CO)_{10}$ on the oxide supports $\gamma$-$Al_2O_3$ and MgO (pretreated by evacuation at 400 °C) were investigated by infrared spectroscopy and other methods. An array of oxidized, neutral, and reduced species was formed in each case as evidenced by $\nu$(CO) IR bands. Supported $Ni(CO)_4$ gave rise to an anionic tricarbonyl species on $\gamma$-$Al_2O_3$ and the high-nuclearity cluster anions $[Ni_5(CO)_{12}]^{2-}$, $[Ni_6(CO)_{12}]^{2-}$, and $[Ni_9(CO)_{18}]^{2-}$ on MgO. Addition of $Mn_2(CO)_{10}$ to $\gamma$-$Al_2O_3$ produced few spectral changes, while $[Mn(CO)_5]^-$ and other surface-substituted manganese carbonyl species resulted on MgO. $[Mn(CO)_5]^-$ on MgO exists as an ion pair with $Mg^{2+}$ unless these sites are blocked. A mechanism, involving a common type of intermediate formed via attack on a CO ligand by a surface oxide, is proposed to explain the variety of surface species observed. This can be used to explain both decarbonylation and redox reactions. Scission of metal-oxygen bonds in the intermediate and subsequent formation of metal-metal bonds also occur to yield metal particles and cluster anions. These processes are particularly favored with the supported nickel carbonyls, consistent with the solution chemistry of these Ni complexes.

## Introduction

Investigations of the chemistry of metal carbonyls at oxide surfaces have disclosed, not surprisingly, that first-row transition-metal carbonyls are more reactive and produce a much more complex array of supported surface carbonyl species than do their second- and third-row congeners.[1-3] Studies of cobalt and iron carbonyls found evidence for valence disproportionation of the parent complexes into cationic and anionic supported metal species. On $Al_2O_3$, MgO, and zeolites, $Co_2(CO)_8$ and $Co_4(CO)_{12}$ reacted with surface oxides ($O_s^-$)[4] to form species proposed to be $Co(CO)_m(O_s)_w$ and $Co(CO)_4^-$.[5-8] Similarly, $Fe(CO)_5$ and $Fe_3(CO)_{12}$ on $Al_2O_3$ yielded $HFe_3(CO)_{11}^-$ as well as zerovalent and oxidized iron centers.[9] Since these observed surface reactions are analogous to those described between the parent complexes and Lewis bases in solution, the possibility arises for similar observations with other supported first-row-metal carbonyl complexes.

In an effort to establish and define trends in the surface reactivities of supported first-row-metal carbonyls, a study of $\gamma$-$Al_2O_3$- and MgO-supported $Ni(CO)_4$ and $Mn_2(CO)_{10}$ was undertaken. Generally, $Ni(CO)_4$ reacts with oxide surfaces to lead to supported zerovalent metal. Parkyns found $Ni(CO)_4$ to be unreactive toward $SiO_2$ but proposed the formation of small metal crystallites upon room-temperature reaction with $Al_2O_3$.[10] Later, the alumina reaction was further characterized and mononuclear subcarbonyl species were proposed as intermediates in the crystallite formation.[11] Nickel metal particles also have been discussed with regard to samples of $Ni(CO)_4$ on MgO.[12]

In the present study, $Ni(CO)_4$ and $Mn_2(CO)_{10}$ on the oxide surfaces were found to undergo reactions analogous to those with

(1) *Tailored Metal Catalysts*; Iwasawa, I., Ed.; D. Reidel: Dordrecht, The Netherlands, 1985.
(2) Hartley, F. R. *Supported Metal Catalysts*; D. Reidel: Dordrecht, The Netherlands, 1986.
(3) *Metal Clusters in Catalysis*; Gates, B. C., Guczi, L., Knozinger, H., Eds.; Elsevier: New York, 1986.
(4) Partially dehydroxylated surfaces will result in the generation of $O_s^-$ and $M^+$ species. The formalism of an $O_s^-$ species is maintained throughout this paper.
(5) Schneider, R. L.; Howe, R. F.; Watters, K. L. *Inorg. Chem.* **1984**, *23*, 4593.
(6) Schneider, R. L.; Howe, R. F.; Watters, K. L. *Inorg. Chem.* **1984**, *23*, 4600.
(7) Gopal, P. G.; Watters, K. L. *Proc. 8th Int. Congr. Catal.* **1984**, *5*, 75.
(8) Connaway, M. C.; Hanson, B. E. *Inorg. Chem.* **1986**, *25*, 1445.
(9) Hanson, B. E.; Bergmeister, J. J., III; Petty, J. T.; Connaway, M. D. *Inorg. Chem.* **1986**, *25*, 3089. Hugues, F.; Smith, A. K.; Ben Taarit, Y.; Basset, J. M.; Commereuc, D.; Chauvin, Y. *J. Chem. Soc., Chem. Commun.* **1980**, 68. Hugues, F.; Bussiere, P.; Basset, J. M.; Commereuc, D.; Chauvin, Y.; Bonneviot, L.; Oliviet, D. *Proc. 7th Int. Congr. Catal.* **1980**, 418.
(10) Parkyns, N. D. *Proc. 3rd Int. Congr. Catal.* **1965**, 914.
(11) Bjorklund, R. B.; Burwell, R. L., Jr. *J. Colloid Interface Sci.* **1979**, 383.
(12) Guglielminotti, E.; Zecchina, A.; Boccuzzi, F.; Borello, E. In *Growth and Properties of Metal Clusters*; Bourdan, J., Ed.; Elsevier: New York, **1980**; pp 165-174. Guglielminotti, E.; Zecchina, A. *J. Mol. Catal.* **1984**, *24*, 331.

0020-1669/89/1328-1236$01.50/0 

Lewis bases in solution but also displayed some properties unique to the surface interactions. The results are discussed in terms of a general reaction scheme for supported first-row carbonyls.

## Experimental Section

$Mn_2(CO)_{10}$ and $Ni(CO)_4$ were purchased from Pressure Chemical Co., Inc., and Strem Chemical, Inc., respectively. $Mn_2(CO)_{10}$ was purified by sublimation, and $Ni(CO)_4$ was used as received. $\gamma$-$Al_2O_3$ ($A_s$ = 188 $m^2/g$) and MgO ($A_s \simeq$ 25 $m^2/g$) were purchased from Akzo Chemie and Cerac, Inc., respectively. Commercial grade CO, $O_2$, and $N_2$ were routinely passed through packed columns of activated zeolite and carbon to remove water and organic impurities. They were further purified by cryostatic distillation methods (−196 °C). Isotopically enriched $^{13}CO$ and $D_2$ were purchased from Prochem, Ltd., and used as received.

Because the experimental procedures have been detailed previously,[5] only a general description is presented here. The powdered oxides were pressed into wafers thin enough to be transparent to infrared radiation from near 1000 to 4000 $cm^{-1}$, 5–10 $mg/cm^2$ (thickness ≃0.3 mm). MgO was used as received for pressing the wafers, but the $\gamma$-$Al_2O_3$ was ground to obtain a fine mesh. Pressures of 30 000 and 7500 psi were used for $\gamma$-$Al_2O_3$ and MgO, respectively. The white wafers were secured in an infrared cell described elsewhere[5] and evacuated while heating to 400 °C. The $\gamma$-$Al_2O_3$ wafers were held at that temperature for 1 h and the MgO wafers for 2 h, times sufficient to remove water from the surfaces as demonstrated by the IR spectra in the 1600–1650- and 3000–4000-$cm^{-1}$ regions. Evacuation of the cell continued as the wafers were allowed to cool to room temperature.

The metal carbonyl complexes were loaded directly onto the oxides in the evacuated cell. For $Mn_2(CO)_{10}$, a small glass chamber, previously charged with crystals of the carbonyl and kept under vacuum, was opened to the wafer, allowing the metal carbonyl vapor to contact the oxide surface. Because $Ni(CO)_4$ has a high vapor pressure at room temperature, an attachment was designed with a small glass bulb calibrated to 2.0 $cm^3$, which fit between the infrared cell and the vacuum system. The attachment was equipped with a three-way stopcock that allowed for charging the glass bulb with a precise, measured pressure of $Ni(CO)_4$ vapor. Because the high-surface-area oxide support comprised over 99% of the surface area in the cell, it may be assumed that all the charged $Ni(CO)_4$ adsorbed on this surface. Solution extraction of supported complexes was accomplished in a $N_2$-filled glovebag with NaCl-saturated anhydrous ethyl ether (Mallinckrodt).

Infared spectra were recorded at room temperature by using Nicolet MX-1 and 10-MX FT-IR spectrometers with a resolution of 2 $cm^{-1}$. Typically, a scan time of 2 min was employed, resulting in 54 scans per spectrum. The sample remained positioned in the IR spectrometer between spectral recordings to ensure reproducible measurement of the sample region. Mass spectra were obtained by transferring gas aliquots to a Hitachi RMU 6D mass spectrometer operating with ionization energy of 10 or 70 eV. The lower energy was used when fragmentation of the parent compound needed to be minimized.

## Results and Discussion

The large number of IR bands displayed by some of the samples precluded experiments employing $^{12}CO/^{13}CO$ isotopic mixtures to identify bands belonging to the same surface species. The interpretation of the IR spectra recorded for the samples of supported $Ni(CO)_4$ and $Mn_2(CO)_{10}$ was accomplished by comparison of the observed IR bands with those previously reported for nickel and manganese surface carbonyl species as well as solid-, solution-, and gas-phase ($Ni(CO)_4$) molecular complexes. Tables I and II list $\nu$(CO) IR bands reported in the literature for nickel and manganese carbonyl species, respectively, that might be responsible for the observed IR bands in the present study.

**$Ni(CO)_4/Al_2O_3$.** IR spectra obtained upon exposure of $Ni(CO)_4$ vapor to a pretreated $\gamma$-$Al_2O_3$ wafer are shown in Figure 1. The spectra shown are for a sample that was 0.8% Ni. The weight percent of nickel was controlled by using the procedure described in the Experimental Section.

The spectrum, recorded immediately after exposure of $Ni(CO)_4$ to $\gamma$-$Al_2O_3$ (Figure 1B), is dominated by a broad band at 2055 $cm^{-1}$ corresponding to the only IR-active band (2057 $cm^{-1}$) for gaseous $Ni(CO)_4$.[10,13] This assignment is supported by the rapid loss of the band under evacuation. Other $\nu$(CO) bands appear in Figure 1B at 1550 (w), 1660 (w), 1840 (m), 1950 (sh), 1995 (sh), 2045 (sh), and 2090 (sh) $cm^{-1}$. These bands are unchanged while the sample remains in a closed cell for up to 30 min.

The bands observed in the present study at 2045 and 2090 $cm^{-1}$ fall into the range of bands reported for terminal CO on Ni(0) particles, while the two bands observed at 1950 and 1995 $cm^{-1}$ correspond to bands that have been assigned to bridging CO on Ni(0) particles.[14,15]

**Table I.** $\nu$(CO) IR Bands for Nickel Species

| sample | $\nu$(CO) freq, $cm^{-1}$ | ref |
|---|---|---|
| | $Al_2O_3$-Supported $Ni(CO)_4$ | |
| $Ni(CO)_4$ on $\gamma$-$Al_2O_3$ | 2055 | |
| $Ni^{2+}$–CO | 2190 | |
| $Ni^{\delta+}$–CO | 2115 | |
| $Ni^0$–CO(term) | 2045, 2090 | |
| $Ni^0_2$–CO(bridge) | 1950, 1995 | |
| $Ni(O_s)(CO)_3^-$ | 1840 | |
| Ni–CO···Al | 1550, 1660 | |
| | MgO-Supported $Ni(CO)_4$ | |
| $Ni(CO)_4$ on MgO | 2058 | |
| $Ni^{\delta+}$–CO | 2125 | |
| $Ni^0$–CO(term) | 2036, 2063 | |
| $Ni^0_2$–CO(bridge) | 1940, 1960 | |
| $[Ni_5(CO)_{12}]^{2-}$ on MgO | 1922, 1979 | |
| $[Ni_6(CO)_{12}]^{2-}$ on MgO | 1790, 1807, 1988 | |
| $[Ni_9(CO)_{18}]^{2-}$ on MgO | 1826, 2001 | |
| | Literature | |
| gaseous $Ni(CO)_4$ | 2057 | 28 |
| $Ni^{2+}$–CO on $Al_2O_3$ | 2190–2200 | 14 |
| $Ni^+$–CO on $Al_2O_3$ | 2130–2160 | 14 |
| $Ni^{\delta+}$–CO on $Al_2O_3$ | 2080–2120 | 14 |
| $Ni^0$–CO(term) | 2020–2090 | 14 |
| $Ni(CO)_3^-$ argon matrix | 1858 | 16 |
| $[Ni_2(CO)_6]^{2-}$ | 1870 | 13 |
| $Li_2[Ni_5(CO)_{12}]$ | 1710 (vw), 1790 (w), 1830 (w), 1920 (m), 1970 (s) | 13 |
| $Li_2[Ni_6(CO)_{12}]$ | 1710 (w), 1790 (m), 1810 (m), 1980 (s) | 13 |
| $[PPh_4]_2[Ni_9(CO)_{18}]$ | 1825 (m), 2005 (s) | 18 |

**Table II.** $\nu$(CO) IR Bands for Manganese Species

| sample | $\nu$(CO) freq, $cm^{-1}$ | ref |
|---|---|---|
| | $\gamma$-$Al_2O_3$-Supported $Mn_2(CO)_{10}$ | |
| $Mn_2(CO)_{10}$ on $\gamma$-$Al_2O_3$ | 2012, 2051 | |
| $Mn^{2+}$–CO | 2193 | |
| Mn–CO···Al | 1695, 1762 | |
| | MgO-Supported $Mn_2(CO)_{10}$ | |
| $Mn_2(CO)_{10}$ on MgO | 1978, 2000, 2052 | |
| $[Mn(CO)_5]^-$ on MgO (weakly interacting) | 1863, 1891 | |
| $[Mn(CO)_5]^-$ on MgO (ion pair with $Mg^{2+}$ sites) | 1800, 1898, 1898, 1916, 2035 | |
| $Mn–CO_2$ (ion pair with $Mg^{2+}$ sites) | 1240 | |
| $Mn^{\delta+}$–CO | 2116 | |
| $Mn^I(O_s)_{6-x}(CO)_x$ ($x$ = 2–4) | 1847, 1910, 1941, 1951, 1960, 2023, 2076 | |
| | Literature | |
| $Mn_2(CO)_{10}$ in THF | 1983 (m), 2013 (s), 2044 (m) | 21 |
| $Mn_2(CO)_{10}$ on $SiO_2$ | 1980 (sh), 2018 (s), 2051 (m) | 20 |
| $HMn(CO)_5$ in THF | 2007 (s), 2016 (vs), 2118 (vw) | 21 |
| $[Mn(CO)_5]^-$ in THF | 1863, 1898 | 23 |
| $Li[Mn(CO)_5]$ in ether (ion pair) | 1781 (s), 1890 (s), 1918 (s), 2013 (m) | 23 |
| $Na[Mn(CO)_5]$ in ether (ion pair) | 1792 (mw), 1887 (s), 1916 (s), 2018 (w) | 23 |
| *trans*-$[Mn(CO)_2(P(OMe)_3)_4]^+$ | 1943 | 30 |
| *cis*-$[Mn(CO)_2(P(OMe)_3)_4]^+$ | 1944 (s), 2000 (s) | 30 |
| *fac*-$[Mn(CO)_3(PEt_3)_3]^+$ | 1943 (s), 2021 (s) | 30 |
| *mer*-$[Mn(CO)_3(PEt_3)_3]^+$ | 1940 (s), 1984 (m), 2020 (w) | 30 |
| *fac*-$[Mn(CO)_3(NH_3)_3]^+$ | 1913 (vs), 2030 (s) | 32 |
| $[Mn(CO)_3(tripod)]^+$ | 1860 (s), 1902 (ms), 1962 (s), 2030 (s) | 33 |
| $[Mn(NCMe)_3(CO)_3]^+$ | 1982, 2060 | 34 |
| $[Mn(PPh_3)_2(CO)_4]^+$ | 2000, 2046 | 35 |

(13) Longoni, G.; Chini, P.; Cavalieri, A. *Inorg. Chem.* **1976**, *15*, 3025. Longoni, G.; Mannassero, M.; Sansoni, M. *J. Organomet. Chem.* **1979**, *174*, 41.

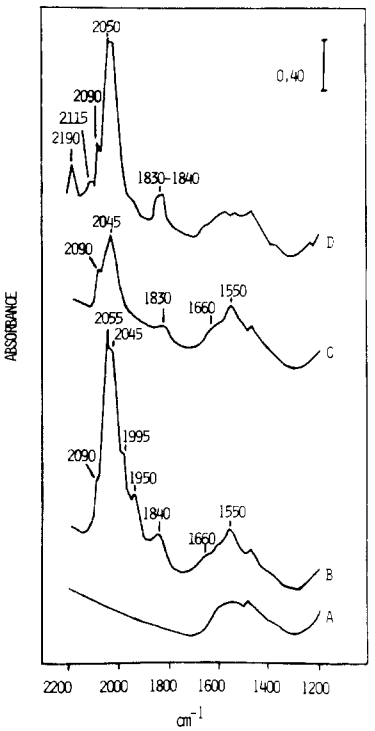


**Figure 1.** Behavior of $\nu$(CO) region of $Ni(CO)_4/Al_2O_3$ (0.8% Ni): (A) $\gamma$-$Al_2O_3$ background after heating to 400 °C for 1 h while evacuating; (B) sample after exposure to $Ni(CO)_4$ in a closed cell; (C) sample after evacuation; (D) sample after addition of 600 Torr of CO.

The band at 1830–1840 $cm^{-1}$ is significantly lower in frequency than any band previously reported for CO adsorbed on supported Ni(0) species. The low frequency suggests a nickel carbonyl species with a reduced metal center, and in fact, the frequency is close to that reported for the anionic complex $Ni(CO)_3^-$ (1858 $cm^{-1}$), which has been isolated in a low-temperature matrix.[16]

No species is identified as being responsible for the bands at 1550 and 1660 $cm^{-1}$ although carbonyl bands in this frequency range have been assigned to M–CO···Al interactions and have been observed for other $Al_2O_3$-supported carbonyl complexes.[17]

Upon a 5-min evacuation of the supported nickel sample (Figure 1C), the band at 2055 $cm^{-1}$ vanishes as do bands at 1995 and 1950 $cm^{-1}$, while the band near 1840 $cm^{-1}$ loses intensity and broadens. Addition of 600 Torr of CO (Figure 1D) leads to reappearance of the band at 2050 $cm^{-1}$ and emergence of new IR bands at 2115 and 2190 $cm^{-1}$. These disappear immediately upon evacuation of CO.

The reactions of $Ni(CO)_4$ with the oxide surface might be expected to produce atomically dispersed nickel. Reaction with added CO provides information about the redox state of this metal through the IR frequencies of the absorbed CO. The two high-frequency $\nu$(CO) bands at 2115 and 2190 $cm^{-1}$, which were only present when the sample was under CO, are assigned to CO on supported nickel. The band at 2190 $cm^{-1}$ is assigned as $Ni^{2+}$–CO[15] on the basis of its easily reversible appearance and of the previous observation of a similar band with samples of $Al_2O_3$–supported nickel prepared from $NiCl_2$ or $Ni(NO_3)_2$.[14] The band at 2115 $cm^{-1}$ lies between those expected for $Ni^+$–CO (2130–2160 $cm^{-1}$) and $Ni^0$–CO (2020–2090 $cm^{-1}$) and, for this reason, has been previously assigned to a monocarbonyl with a partially oxidized metal center, $Ni^{\delta+}$–CO.[14]

**$Ni(CO)_4/MgO$.** $Ni(CO)_4$ loaded onto pretreated MgO continues to react for several hours after the initial exposure. Infrared spectra were recorded immediately, 15 min, 1 h, and 24 h after loading a sample, which was 1.0% Ni (Figure 2a(B–E)). The reactivity of $Ni(CO)_4$ on magnesia is greatly increased as compared to that on $\gamma$-alumina, which is evident from the rich $\nu$(CO) region of the IR spectra.

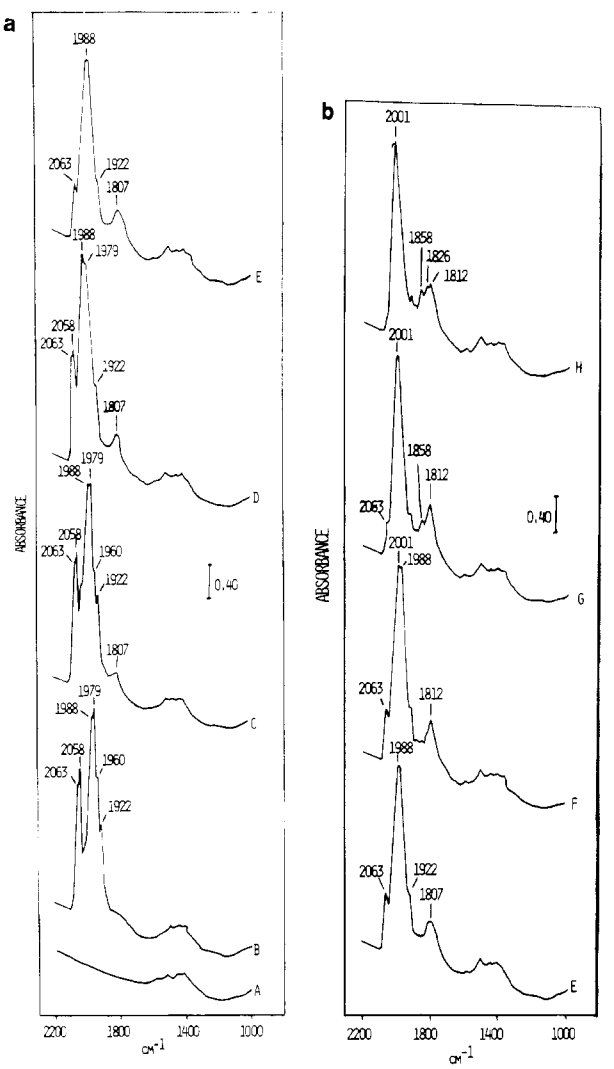


**Figure 2.** (a) Behavior of $\nu$(CO) region of $Ni(CO)_4/MgO$ (1.0% Ni): (A) MgO background after heating to 400 °C for 2 h while evacuating; (B) sample immediately after exposure to $Ni(CO)_4$ in a closed cell; (C) sample 15 min later; (D) sample 1 h later; (E) sample 24 h later. (b) Behavior of $\nu$(CO) region of $Ni(CO)_4/MgO$ (1.0% Ni): (E) sample 24 h after addition of $Ni(CO)_4$; (F) sample after evacuation for 10 s; (G) sample after evacuation for 1 min; (H) sample after evacuation for 10 min.

The band initially evident at 2058 $cm^{-1}$ loses intensity over the first 1 h and then vanishes after several hours. By analogy to the $\gamma$-$Al_2O_3$ system, this band is assigned to the physisorbed $Ni(CO)_4$, though it is not nearly as intense upon immediate $Ni(CO)_4$ adsorption as was the case on $\gamma$-$Al_2O_3$. In fact, Figure 2a(B) is dominated by a pair of bands at 1979 and 1988 $cm^{-1}$ with a shoulder at 2063 $cm^{-1}$ and weaker bands at 1922 and 1960 $cm^{-1}$. During the first 1 h after loading, the intensities of the 1922- and 1979-$cm^{-1}$ bands diminish, concomitant with an increase in the band at 1988 $cm^{-1}$; also, a band at 1807 $cm^{-1}$ with a shoulder at 1790 $cm^{-1}$ emerges. These spectral changes continue for several hours, after which no further changes are observed. Figure 2a(E) shows the spectrum recorded after the sample remained in a closed cell for 24 h. Similar spectral observations were made for samples that were 0.1, 0.2, 0.4, 0.6, and 0.8% Ni, except no $\nu$(CO) band indicating physisorbed $Ni(CO)_4$ was apparent for the three lower loadings.

The bands in the 1700–2000-$cm^{-1}$ region are discussed in order of their appearance after the initial loading of $Ni(CO)_4$. The two bands at 1922 and 1979 $cm^{-1}$ match well the medium and strong $\nu$(CO) bands for the pentanuclear cluster anion $[Ni_5(CO)_{12}]^{2-}$ (1920 (m) and 1970 (s) $cm^{-1}$).[13] The assignment of the 1922-

(14) Peri, J. B. *J. Catal.* **1984**, *86*, 84.
(15) Peri, J. B. *Discuss. Faraday Soc.* **1966**, *41*, 121.
(16) Breeze, P. A.; Burdett, J. K.; Turner, J. J. *Inorg. Chem.* **1981**, *20*, 3369.
(17) Brown, T. L. *J. Mol. Catal.* **1981**, *12*, 41.

and 1979-$cm^{-1}$ bands to the anionic $Ni_5$ cluster is supported by extraction of the complex from the MgO surface. In a $N_2$-filled glovebag, a NaCl-saturated ether solution was used to wash the pellet. The IR spectrum of the solution matched the published solution spectrum of $[Ni_5(CO)_{12}]^{2-}$.[13]

The intensity of the bands due to the $Ni_5$ cluster on the MgO surface is greatest immediately after $Ni(CO)_4$ loading, but they diminish and disappear as the sample is left in a closed cell. The three $\nu$(CO) bands (1790, 1807, and 1988 $cm^{-1}$), which emerge and grow more intense until they dominate the $\nu$(CO) region, match the medium and strong bands reported for the hexanuclear anionic cluster $[Ni_6(CO)_{12}]^{2-}$ (1790 (m), 1810 (m), and 1980 (s) $cm^{-1}$).[13]

Subsequent room-temperature evacuation of the $Ni(CO)_4/MgO$ samples facilitates further changes in the $\nu$(CO) IR region, shown in Figure 2b(E–H). A very brief evacuation (10 s) leads to the spectrum in Figure 2b(F) displaying a new band at 2001 $cm^{-1}$, which remains unchanged after $1^1/_2$ h in a closed cell. Evacuation for longer periods sharpens the new band and results in the emergence of bands at 1812, 1826, and 1858 $cm^{-1}$ at the expense of the other bands in the region (Figure 2b(F–H)). These results indicate $[Ni_9(CO)_{18}]^{2-}$ (1825 (m) and 2005 (s) $cm^{-1}$) has been formed.[18]

Exposure of the samples to 600 Torr of CO alters some $\nu$(CO) frequencies and reduces the intensity of the preexisting $\nu$(CO) bands, while additional bands are unmasked at 1940 and 2036 $cm^{-1}$. Samples *not* evacuated prior to CO exposure display an additional band at 2125 $cm^{-1}$ not observed for samples exposed to CO after evacuation, but this new band gradually loses intensity along with the other bands in the spectrum as the sample remains under CO. Mass spectra of the gas phase above the sample, after CO exposure, show the presence of gaseous $Ni(CO)_4$, indicating Ni surface species have been converted back to gaseous $Ni(CO)_4$. This explains the general loss of intensity of the surface $\nu$(CO) bands. Frequencies observed at 1940, 1960, 2036, and 2063 $cm^{-1}$ do not match any bands of molecular nickel complexes; bands at 1940 and 1960 $cm^{-1}$ are assigned to bridging CO on Ni(0) particles, and bands at 2036 and 2063 $cm^{-1}$ are assigned to terminal CO on Ni(0). The frequencies for both the bridging and terminal CO groups on Ni(0) are shifted downward from those observed for the same species on $\gamma$-alumina (1950, 1995 $cm^{-1}$ and 2045, 2090 $cm^{-1}$, respectively), reflecting the more basic nature of the magnesia support. The band at 2125 $cm^{-1}$ is assigned to a monocarbonyl with a partially oxidized metal center as for $Ni(CO)_4/Al_2O_3$, but no band around 2190 $cm^{-1}$ ($Ni^{2+}$–CO) is observed.

Exposure of 50 Torr of THF vapor to a sample displaying a spectrum like that in Figure 2a(E) results in the disappearance of the band at 2063 $cm^{-1}$ and facilitates no other major changes except to sharpen significantly the bands at 1790 (sh), 1807, and 1988 $cm^{-1}$. Tetrahydrofuran has been shown to coordinate unsaturated magnesium sites and prevent interactions between carbonyl oxygens and the surface Lewis acid sites.[19] Therefore, the disappearance of the 2063-$cm^{-1}$ band is evidence that a Ni–CO species was bonded to a $Mg^{2+}$ site.

The $\nu$(OH) IR region was also monitored during all experiments. Pretreated MgO displays a strong, sharp band at 3756 $cm^{-1}$ assigned to the isolated, terminal O–H stretch. After $Ni(CO)_4$ exposure, the band broadens considerably on the low-frequency side, indicative of weak hydrogen-bonding interactions between the hydroxyl groups and the nickel species. Upon exposure to CO, the $\nu$(OH) band narrows and intensifies to its original contour, concomitant with the decrease in the $\nu$(CO) bands and formation of gas-phase $Ni(CO)_4$.

**$Mn_2(CO)_{10}/Al_2O_3$.** $Mn_2(CO)_{10}$ was deposited via room-temperature sublimation (30–45 s) onto pretreated $\gamma$-$Al_2O_3$ infrared wafers. The IR spectrum recorded immediately after loading is shown in Figure 3B. Much of the $Mn_2(CO)_{10}$ that is loaded on $\gamma$-$Al_2O_3$ seems to remain as the physisorbed complex. The two

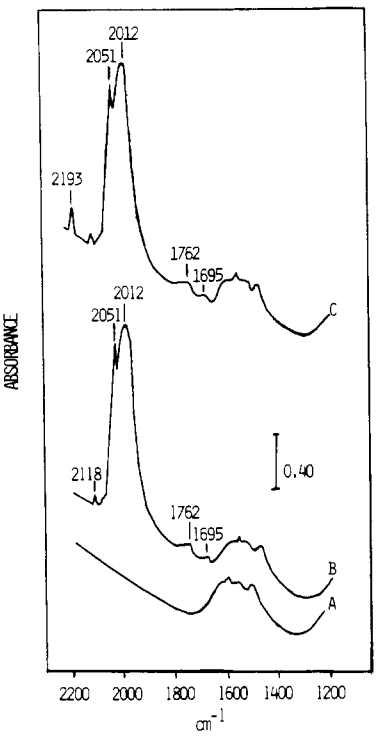


**Figure 3.** Behavior of $\nu$(CO) region of $Mn_2(CO)_{10}/Al_2O_3$: (A) $\gamma$-$Al_2O_3$ background after heating to 400 °C for 1 h while evacuating; (B) sample immediately after a 45-s exposure to $Mn_2(CO)_{10}$ vapor in a closed cell; (C) sample after exposure to 600 Torr of CO.

most intense $\nu$(CO) bands, at 2012 and 2051 $cm^{-1}$, have been observed for $Mn_2(CO)_{10}$ physisorbed on $SiO_2$ and correspond well to the two most intense $\nu$(CO) bands of the molecular complex (2013 and 2044 $cm^{-1}$).[20,21] The band at 2012 $cm^{-1}$ is much broader than the corresponding band for $Mn_2(CO)_{10}/SiO_2$ or molecular $Mn_2(CO)_{10}$ and may obscure the weaker band at ~1980 $cm^{-1}$ normally observed for molecular $Mn_2(CO)_{10}$. This broadening is typical of metal carbonyl spectra on alumina. Other weak bands are present in the spectrum at 1695, 1762, and 2118 $cm^{-1}$.

It should be added that axially substituted $Mn_2(CO)_9L$ species have $\nu$(CO) spectra with intense bands near 2010 and 2040 $cm^{-1}$ and a very weak band near 2110 $cm^{-1}$. It is conceivable that some or all of the surface manganese carbonyl is bonded to aluminum ions at the surface of the alumina through the oxygen of a carbonyl in the axial position. This would produce a $Mn_2(CO)_9L$ type species that might have a very weak band at 2118 $cm^{-1}$ as well as at least one weak lower frequency band in the 1700–1800-$cm^{-1}$ region.[22]

Evacuation and subsequent addition of 600 Torr of CO to $Mn_2(CO)_{10}/Al_2O_3$ produces no changes in the $\nu$(CO) IR region except the appearance of a band at 2193 $cm^{-1}$ (Figure 3C). This surface carbonyl species is stable only under a CO atmosphere since it reversibly vanishes and reappears with each subsequent evacuation/carbonylation cycle. This band may be assigned to CO adsorbed to $Mn^{2+}$ ions.

**$Mn_2(CO)_{10}/MgO$.** Infrared spectra for $Mn_2(CO)_{10}$ adsorbed on pretreated MgO are shown in Figure 4, and as for $Ni(CO)_4$ samples, $Mn_2(CO)_{10}$ supported on magnesia produces IR spectra richer in $\nu$(CO) bands than does $Mn_2(CO)_{10}$ on $\gamma$-alumina. Immediately after loading, a composite of bands is present in the 1800–2100-$cm^{-1}$ region with at least nine frequencies clearly discernable (Figure 4B) and the metal carbonyl surface species continue to react for up to 24 h in the closed cell (Figure 4C,D).

Immediately after loading, three bands that indicate the presence of the physisorbed parent carbonyl (1978, 2000, and 2052

(18) Longoni, G.; Chini, P. *Inorg. Chem.* **1976**, *25*, 3029.
(19) Lamb, H. H.; Gates, B. C. *J. Am. Chem. Soc.* **1986**, *108*, 81.
(20) Keyes, M. P. Ph.D. Thesis, University of Wisconsin—Milwaukee, 1986.
(21) *Transition Metal Hydrides*; Muetterties, E. L., Ed.; Marcel Dekker: New York, 1971.
(22) Haas, H.; Sheline, R. K. *J. Chem. Phys.* **1967**, *47*, 2996.

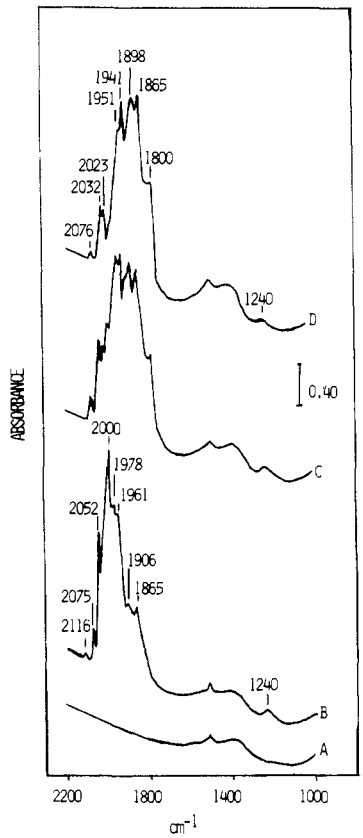


**Figure 4.** Behavior of $\nu$(CO) region of $Mn_2(CO)_{10}$/MgO: (A) MgO background after heating to 400 °C for 2 h while evacuating; (B) sample immediately after a 45-s exposure to $Mn_2(CO)_{10}$ vapor in a closed cell; (C) sample after 3 h; (D) sample after 24 h.

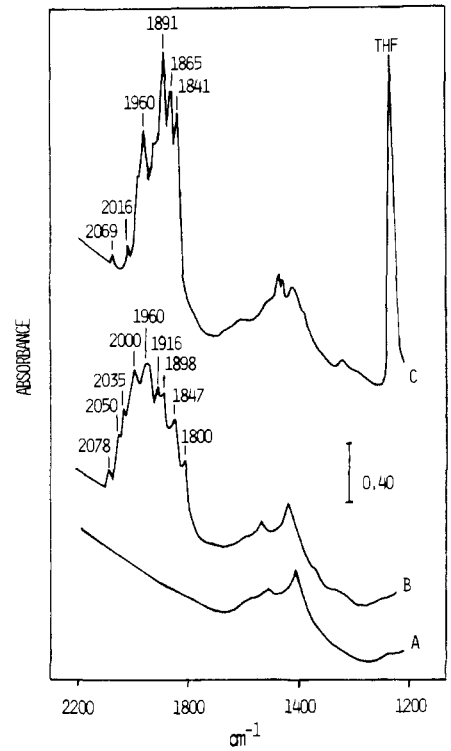


**Figure 5.** Behavior of $\nu$(CO) region of $Mn_2(CO)_{10}$/MgO: (A) MgO background after heating to 400 °C for 2 h while evacuating; (B) sample 2 h after exposure to $Mn_2(CO)_{10}$ vapor in a closed cell; (C) sample after addition of 50 Torr of THF.

$cm^{-1}$)[21] are present. The three $\nu$(CO) bands assigned to physisorbed $Mn_2(CO)_{10}$ diminish and vanish in a few hours, concomitant with the emergence and growth of new bands. Throughout the changes described for the $\nu$(CO) IR bands, one band at 1240 $cm^{-1}$ becomes apparent immediately after loading (Figure 4B) and grows to a maximum intensity in 6–8 h (Figure 4C), after which it steadily decreases until it vanishes 24 h after loading (Figure 4D). Bands at 2076 and 2116 $cm^{-1}$ show the same pattern; the behavior suggests an intermediate in the surface reaction of $Mn_2(CO)_{10}$.

Along with the bands immediately apparent for $Mn_2(CO)_{10}$ are four bands at 1800, 1898, 1916, and 2035 $cm^{-1}$ (best seen in Figure 5B) matching those reported for ion pairs between $M^+$ (M = Na, Li) and $[Mn(CO)_5]^-$ ions in solution (Table II).[23] In the solution studies, $Mg^{2+}$ and other cations were found to interact with an axial CO ligand of $[Mn(CO)_5]^-$, resulting in an overall $C_{3v}$ symmetry and four IR-active $\nu$(CO) bands. The pretreatment of the MgO in the present study is expected to yield $Mg^{2+}$ surface sites that would be available for such interactions. Tetrahydrofuran has been shown to coordinate unsaturated magnesium sites and prevent ion-pair interactions as in the proposed $Mg^{2+}[Mn(CO)_5]^-$ surface species.[19] Addition of 50 Torr of THF to a sample with the apparent surface ion pair results in the four bands assigned to this species being replaced by bands at 1865 and 1891 $cm^{-1}$ (Figure 5C). These new bands may indicate the presence of $[Mn(CO)_5]^-$ that is "solvent separated" from the $Mg^{2+}$ sites.[21] Bands at 2000 and 2052 $cm^{-1}$ also vanish, suggesting the adsorption of THF facilitates the reaction of physisorbed $Mn_2(CO)_{10}$.

Although the major features of the spectra are reproducible over many samples, different samples identically prepared lead to slightly different relative intensities. Due to the abundance of IR bands, it is not possible to identify allometric correspondence between pairs or groups of bands. Lower loadings of $Mn_2(CO)_{10}$ neither aid the resolution of the bands nor significantly affect the rate of disappearance of the $\nu$(CO) bands assigned to physisorbed $Mn_2(CO)_{10}$. Little can be done experimentally to affect the course of spectral changes shown in Figure 4. Neither room-temperature evacuation for up to 30 min nor addition of 600 Torr of CO seems to affect the intensity loss of the $\nu$(CO) bands assigned to physisorbed $Mn_2(CO)_{10}$ or the emergence and growth of other IR bands present.

The remainder of the bands seen in Figures 4 and 5 at 1841, 1906, 1941, 1961, 2023, and 2032 $cm^{-1}$ may indicate the presence of various di-, tri-, and tetracarbonyls with +1 manganese centers, $[Mn^+(CO)_x(O_s)_{6-x}]$ (where $x$ = 2–4). Analogous oxidized carbonyl species were proposed with supported cobalt by starting from $Co_2(CO)_8$ and $Co_4(CO)_{12}$.[5-7] The formation of such species is consistent with the known reactions of $Mn_2(CO)_{10}$ with Lewis bases. Infrared carbonyl frequencies for various molecular cationic manganese carbonyl species are given in Table II for comparison with the ones obtained in the present study.

**Surface Processes: Supported $Ni(CO)_4$.** Our results, though more detailed, are consistent with those of Parkyns and other previous studies of oxide-supported $Ni(CO)_4$.[10-12] Reaction of $Ni(CO)_4$ with $\gamma$-$Al_2O_3$ leads to the formation of metallic nickel particles and surface-bonded nickel carbonyls. We believe a single reaction mechanism can be used to explain the interactions of $Ni(CO)_4$ with both MgO and $\gamma$-$Al_2O_3$. In both cases, the reaction sequence could be initiated by a nucleophilic attack by a surface oxide on a carbonyl ligand to form an oxycarbonyl species, which leads to elimination of one of the remaining CO ligands. Subsequent migration of the surface oxide yields $Ni(O_s)(CO)_3^-$ (**1**)

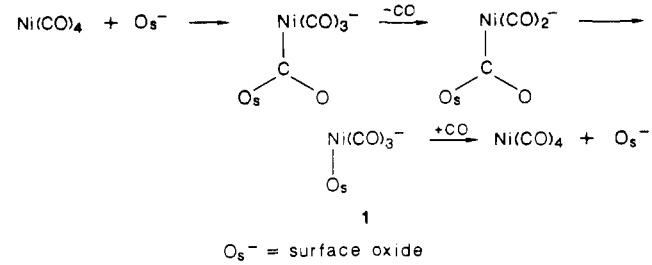


1

$O_s^-$ = surface oxide

(IR $\nu$(CO) on $\gamma$-$Al_2O_3$ is 1840 $cm^{-1}$). This reaction type has been

(23) Pribula, C. D.; Brown, T. L. *J. Organomet. Chem.* **1974**, *71*, 415.

**Scheme I**

$Ni(CO)_4$ on $\gamma$-$Al_2O_3$ and MgO:

$$n\underset{\underset{Os}{|}}{Ni(CO)_3^-} \longrightarrow Ni_n(CO)_y + (3n-y)CO + nOs^- \quad (I.1)$$

1

$Ni(CO)_4$ on MgO:

$$1 \xrightarrow{-CO} \underset{\underset{Os}{|}}{Ni(CO)_2^-} \xrightarrow[5Ni(CO)_4]{} [Ni_5(CO)_{12}]^{2-} + \underset{\underset{Os}{|}}{Ni^+} + 10CO \quad (I.2)$$

2

$$[Ni_5(CO)_{12}]^{2-} + Ni(CO)_4 \longrightarrow [Ni_6(CO)_{12}]^{2-} + 4CO \quad (I.3)$$

$$[Ni_5(CO)_{12}]^{2-} + Ni^0 \longrightarrow [Ni_6(CO)_{12}]^{2-} \quad (I.4)$$

$$[Ni_5(CO)_{12}]^{2-} + Ni_n(CO)_y \longrightarrow [Ni_6(CO)_{12}]^{2-} + Ni_{n-1}(CO)_{y-x} + xCO \quad (I.5)$$

$$3[Ni_6(CO)_{12}]^{2-} + Ni^{2+} \longrightarrow 2[Ni_9(CO)_{18}]^{2-} + Ni^0 \quad (I.6)$$

described for group VI carbonyls with surface oxides of $Al_2O_3$ and with Lewis bases in solution and in the gas phase.[17,24-26]

Scheme I shows the series of reactions proposed between $Ni(CO)_4$ and the supports, $\gamma$-$Al_2O_3$ and MgO. As shown in Scheme I, species **1** may react in two ways. First, Ni(0) particles may be formed by scission of the Ni–$O_s$ bonds and formation of Ni–Ni bonds, in small clusters, releasing CO (reaction I.1). Metallic Ni particles with terminal and bridging adsorbed CO were identified with samples of $Ni(CO)_4$ on both $\gamma$-$Al_2O_3$ and MgO. Second, $Ni(O_s)(CO)_2^-$ (**2**) may be formed on the more basic magnesia from the loss of a CO ligand, similar to the formation of **1**. Species **2** is a possible intermediate in the formation of the high-nuclearity anionic clusters that were identified on MgO (reactions I.3–I.6). This is analogous to gas-phase reactions of $Fe(CO)_5$ with relatively strong Lewis bases that result in the release of two CO groups (reaction I.2).[25] Possibly due to the high reactivity, the electron-deficient species **2** was not directly observed.

The reaction of $Ni(CO)_4$ with MgO to form nickel cluster anions parallels the reaction of the parent carbonyl in basic solutions.[27] Recent studies have more fully characterized the anionic clusters;[18,28] in nonaqueous solutions of alkali-metal hydroxides, $Ni(CO)_4$ reacts to form $[Ni_5(CO)_{12}]^{2-}$, analogous to our observation of the $Ni_5$ cluster on MgO. In the basic solutions, $[Ni_5(CO)_{12}]^{2-}$ was found to further convert to a hexanuclear cluster:

$$[Ni_5(CO)_{12}]^{2-} + Ni(CO)_4 \rightarrow [Ni_6(CO)_{12}]^{2-} + 4CO$$

This reaction is analogous to the formation of $[Ni_6(CO)_{12}]^{2-}$ on MgO at the expense of the pentanuclear cluster. The Ni(0) particles formed in eq I.1 also may react with $[Ni_5(CO)_{12}]^{2-}$ to form the hexanuclear cluster. Three possible reactions forming the hexanuclear cluster from the pentanuclear cluster are given in Scheme I (eq I.3–I.5).

In solution, $[Ni_9(CO)_{18}]^{2-}$ forms by a redox reaction with $Ni^{2+}$ ions:

$$3[Ni_6(CO)_{12}]^{2-} + NiCl_2 \rightarrow 2[Ni_9(CO)_{18}]^{2-} + Ni^0 + 2Cl^-$$

A similar reaction can produce the nonanuclear cluster on MgO by the consumption of surface $Ni^{2+}$ species by the hexanuclear nickel cluster. When a sample displaying $\nu$(CO) bands assigned to $[Ni_6(CO)_{12}]^{2-}$ is exposed to CO, oxidized nickel species are present (2125 $cm^{-1}$). However, when a similar sample is evacuated to generate supported $[Ni_9(CO)_{18}]^{2-}$, which is then exposed to CO, the $\nu$(CO) band due to the oxidized nickel species is not observed. This result is consistent with the consumption of the oxidized nickel in the formation of $[Ni_9(CO)_{18}]^{2-}$ (Scheme I, reaction I.6).

**Scheme II**

$Mn_2(CO)_{10}$ on $\gamma$-$Al_2O_3$ and MgO:

$$\underset{\underset{Mn(CO)_4}{|}\\\underset{Os}{|}}{Mn(CO)_5^-} + Os^- \longrightarrow \underset{\underset{(Os)_2}{|}}{[Mn^I(CO)_4]^-} + [Mn(CO)_5]^- \quad (II.1)$$

3 4

$Mn_2(CO)_{10}$ on $\gamma$-$Al_2O_3$:

$$\underset{\underset{2Os}{|}}{\overset{\overset{H}{|}}{2}4} \longrightarrow Mn^{2+} + 4CO + 4Os^- + H_2 \quad (II.2)$$

$Mn_2(CO)_{10}$ on MgO:

$$4 + nOs^- \longrightarrow \underset{\underset{(Os)_{n+2}}{|}}{Mn^I(CO)_{4-n}} + nCO \quad (II.3)$$

**Surface Processes: Supported $Mn_2(CO)_{10}$.** The transformations that $Mn_2(CO)_{10}$ undergoes on $\gamma$-$Al_2O_3$ and MgO parallel the reactions of the carbonyl complex with Lewis bases in solution.[29] When $Mn_2(CO)_{10}$ is reacted in solution with O-, N-, and P-containing compounds, valence disproportionation occurs to yield $[Mn(CO)_5]^-$ and $[Mn(CO)_xL_{6-x}]^{n+}$, where $x$ = 0–4. The exact cationic product formed depends in part on the strength of the base and on the reaction conditions.[30] While it remains difficult to elucidate the mechanism of these reactions in solution, the formation of cationic and anionic species with samples of supported $Mn_2(CO)_{10}$ may be understood in the context of an initial nucleophilic attack by a surface oxide on one of the CO ligands to produce oxycarbonyl species. Due to the ionic nature of MgO, the resulting complex exists on MgO as an ion pair where the support cation, $Mg^{2+}$, is interacting with the $-CO_2$ group and may be responsible for the IR band observed at 1240 $cm^{-1}$ for $Mn_2(CO)_{10}$/MgO. As demonstrated with supported nickel, evolution of CO, migration of the surface oxide, and formation of a metal–oxide bond follows to yield **3**. The coordinated surface oxide

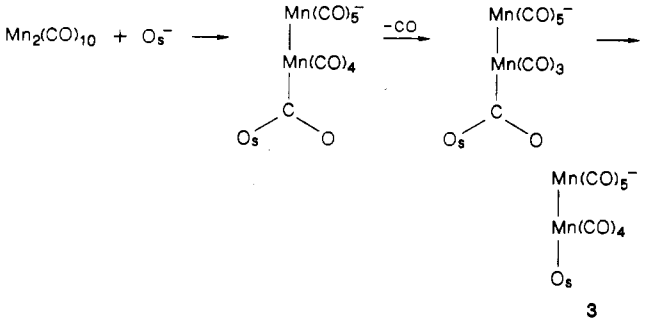


3

causes charge separation in the dinuclear carbonyl species with the electron density polarized away from the surface, as shown for **3**, resulting in heterolytic scission of the Mn–Mn bond to yield $[Mn(CO)_5]^-$ and **4**, as seen in Scheme II (reaction II.1). On $\gamma$-$Al_2O_3$, species **4** may react with surface hydroxyl groups to oxidize Mn(I) to Mn(II) with evolution of CO and $H_2$ (reaction II.2), as shown with other $Al_2O_3$-supported carbonyls.[1-3] Carbon monoxide bound to Mn(II) was not observed when MgO was the support, indicating the surface hydroxyl groups on MgO are not acidic enough to allow the reaction between $H^+$ and Mn(I). However, the more strongly basic surface oxides on MgO liberate additional CO ligands from the manganese cation, as occurs with supported $Ni(CO)_4$ and $Fe(CO)_5$, to produce di-, tri-, and tet-

(24) Lichtenberger, D. L.; Brown, T. L. *J. Am. Chem. Soc.* **1978**, *100*, 306 and references therein.
(25) Lane, K. R.; Sallans, L.; Squires, R. R. *J. Am. Chem. Soc.* **1986**, *108*, 4368.
(26) Laniecki, M.; Burwell, R. L. *J. Colloid Interface Sci.* **1980**, *75*, 95.
(27) Hieber, W.; Ellerman, J.; Zahn, E. *Z. Naturforsch., B* **1963**, 589.
(28) Braterman, P. S. *Metal Carbonyl Spectra*; Academic Press: New York, 1975.
(29) *Comprehensive Organometallic Chemistry*; Wilkinson, G., Stone, F. G. A., Abel, E. W., Eds.; Pergamon Press: New York, 1982; Vol. 4.
(30) Hieber, W.; Beck, W.; Zeitler, G. *Angew. Chem.* **1963**, *73*, 364.

racarbonyl surface species (reaction II.3).

## Conclusions

Detailed interactions of $Ni(CO)_4$ and $Mn_2(CO)_{10}$ with both $\gamma$-$Al_2O_3$ and MgO are shown to include the formation of oxidized, reduced, and zerovalent metal surface species. It is proposed that the reactions are initiated by attack at one of the carbonyl ligands of the parent complex by support surface oxides to form oxycarbonyl ligands. The remaining carbonyl ligands then become labile toward dissociation and rearrangement to give a variety of surface carbonyls.

Disparate reactivities of the surface carbonyl species are observed on the different supports. In a comparison of the two oxide supports MgO and $\gamma$-$Al_2O_3$, MgO is shown to induce more complete CO dissociation. This results in a larger range of surface species for the MgO-supported carbonyls, including di-, tri-, and tetracarbonyl surface species for $Mn_2(CO)_{10}$/MgO and high-nuclearity carbonyl anions for $Ni(CO)_4$/MgO.

Two major differences are apparent in the reactivities of $Mn_2(CO)_{10}$ and $Ni(CO)_4$ toward the supports. First, metal–metal bond formation occurs to a much greater extent for samples derived from supported $Ni(CO)_4$. The presence of metal particles is shown with $Ni(CO)_4$ on both $\gamma$-$Al_2O_3$ and MgO but not with supported $Mn_2(CO)_{10}$. Further, metal–metal bonds in the cluster anions are formed with samples of $Ni(CO)_4$/MgO. Scheme I shows how the cluster anions might serve as intermediates in the formation of Ni particles on this support.

Second, metal–oxygen bonds between metal subcarbonyl species and the supports seem to be formed and retained to a greater extent with supported $Mn_2(CO)_{10}$ than with $Ni(CO)_4$. There is evidence for the series of species $Mn(CO)_x(O_s)_{6-x}$ on MgO, but no analogous species are identified with $Ni(CO)_4$/MgO samples. Again, this observation is entirely consistent with the "softer" nature of Ni as opposed to that of Mn in reactions with bases.

Formation of reduced, oxidized, and zerovalent metal species seems to be characteristic of oxide-supported first-row-metal carbonyls. Iron pentacarbonyl is reported to form $Fe^{2+}$, $[HFe_3(CO)_{11}]^-$, and metallic iron.[9] Reactions of $Co_2(CO)_8$ with oxide surfaces lead to $Co(CO)_x(O_s)_y$ species along with the anion $[Co(CO)_4]^-$ and, at least on MgO, small cobalt particles.[5-7] These redox reactions presumably are similar to those in Schemes I and II. The array of metal species and oxidation states observed when first-row carbonyl complexes contact oxide surfaces is in considerable contrast with the reactions of second- and third-row transition-metal carbonyls on these surfaces.[1-3,5,31] This is not surprising in view of the propensity of first-row-metal carbonyls to disproportionate to form anions and cations. The large degree of charge separation at the oxide surfaces naturally favors disproportionation to charged species where possible, as well as formation of metal particles in which charge separation is quite facile.

Finally, it is important to note the facile nature of these reactions. The fact that some of the molecular metal carbonyl surface species observed may interconvert with supported metallic particles via reaction pathways and equilibrium states suggest the difficulty of determining the true nature of the catalytic species in reactions over oxide-supported first-row metals under carbonylation conditions.

**Acknowledgment.** We wish to thank the Laboratory for Surface Studies, UW—Milwaukee, for generous support of this research.

**Registry No.** $Al_2O_3$, 1344-28-1; MgO, 1309-48-4; $Ni(CO)_4$, 13463-39-3; $Mn_2(CO)_{10}$, 10170-69-1; $[Ni_5(CO)_{12}]^{2-}$, 56938-71-7; $[Ni_6(CO)_{12}]^{2-}$, 52261-68-4; $[Ni_9(CO)_{18}]^{2-}$, 60475-87-8; $[Mn(CO)_5]^-$, 14971-26-7; $^{13}C$, 14762-74-4.

(31) Keyes, M. P.; Watters, K. L. *J. Catal.* **1988**, *110*, 96. Smith, A. K.; Hugues, F.; Theolier, A.; Basset, J. M.; Ugo, R.; Zanderighi, G. M.; Bilhou, J. L.; Bilhou-Bougnol, V.; Graydon, W. F. *Inorg. Chem.* **1979**, *18*, 3104. Tanaka, K.; Watters, K. L.; Howe, R. F. *J. Catal.* **1982**, *75*, 23. Watters, K. L.; Howe, R. F.; Chojnacki, T. P.; Fu, C. M.; Schneider, R. L.; Wong, N. B. *J. Catal.* **1980**, *66*, 424.

(32) Herberhold, M.; Wehrmann, F.; Neugerbauer, D.; Huttner, G. *J. Organomet. Chem.* **1978**, *152*, 329.

(33) Stiegman, A. E.; Goldman, A. S.; Philbin, C. E.; Tyler, D. R. *Inorg. Chem.* **1986**, *27*, 2976.

(34) Treichel, P. M.; Direen, G. F.; Mueh, H. J. *J. Organomet. Chem.* **1972**, *44*, 339.

(35) Narayanan, B. A.; Amatori, C.; Kochi, J. K. *Organometallics* **1987**, *6*, 129.